# Ground-State Atomic Nitrogen Measurements using fs-TALIF in High-Pressure NRP Discharges

Ciprian Dumitrache, Arnaud Gallant, Gabi D. Stancu, Christophe O Laux

AIAA SciTech Forum
6-10 January 2020, Orlando, FL
AIAA Scitech 2020 Forum

10.2514/6.2020-1745



# Ground-State Atomic Nitrogen Measurements using fs-TALIF in High-Pressure NRP Discharges

Ciprian Dumitrache[1], Arnaud Gallant[2], Gabi Daniel Stancu[3], Christophe Laux[4]
*Laboratoire EM2C, CNRS, CentraleSupélec, Université Paris-Saclay, 91190 Gif-sur-Yvette, France*

**Measurements of ground state atomic nitrogen inside of a nanosecond repetitively pulsed (NRP) discharge operating at pressures between 0.1-5 bar are performed using a femtosecond two-photon absorption laser induced fluorescence (fs-TALIF) technique. The main goal of this work is to develop a quench-free diagnostic technique which would allow measurements at elevated pressures with high spatial and temporal resolution. Quantitative information is extracted from the TALIF signal via a novel calibration technique based on direct absorption measurements performed in a low-pressure DC discharge. The VUV measurements were done at the Soleil synchrotron facility using their unique high-resolution Fourier-transform spectrometer ($\lambda/\Delta\lambda = 10^{16}$). During this preliminary work, fs-TALIF measurements of N($^4$S) are demonstrated in the post-discharge of the NRP between 1-500 µs after the nanosecond pulse. A maximum number density of N-atoms of $5 \times 10^{16}\ cm^{-3}$ was measured at 1 µs after the pulse when the discharge was operated at 1 bar in pure nitrogen. Importantly, the limit of detection of the fs-TALIF technique was determined to be $n_{N(^4S)} \sim 10^{12}\ cm^{-3}$. This is approximately two orders of magnitude lower than previously reported by ns-TALIF.**

## I. Introduction

Atomic nitrogen obtained by efficient dissociation in a nanosecond pulsed repetitively pulsed (NRP) discharge can be useful for many industrial applications such as the enhancement of nitridation processes[1], the synthesis of novel nanomaterials[2] or biomedical treatment[3,4]. Additionally, understanding the kinetics of atomic nitrogen production at high-pressure conditions (above 1 bar) can be used to better understand the plasma influence on $NO_x$ generation in plasma-assisted combustion applications[5,6]. Nonetheless, measurements of the ground-state atomic nitrogen are challenging to perform because the excitation photon energy lies in the VUV range ($\lambda$ =100-120 nm) which is not readily accessible by traditional laser systems.

Past studies employed VUV direct absorption spectroscopy to overcome this difficulty. For example, Niemi et al.[7] have used the DESIR beamline from the Soleil Synchrotron facility to measure atomic nitrogen and atomic oxygen production in a radio-frequency (rf) discharge which was operated in a mixture consisting of air diluted with helium. They reported a maximum N-atom concentration of $5.7 \pm 0.4 \times 10^{13}$ cm$^{-3}$ at 1 bar in a mixture containing 0.1% of air (by volume). While such a technique works well for steady state and uniform discharges, it cannot be used easily in NRPs due to its lack of spatial and temporal resolution. An indirect measurement of N($^4$S) in the post-discharge that partially overcomes this issue was introduced by Salmon[8]. According to the author, the three-body recombination reaction: $N\ (^4S) + N\ (^4S) + M \underset{k_2}{\overset{k_1}{\rightleftharpoons}} N_2\ (B^3\Pi_g,\ v = 11) + M$ is in partial equilibrium in the post-discharge. Therefore, an indirect measurement of ground-state atomic nitrogen can be obtained by observing the emission from the $N_2$(B,v=11) state (first positive). Gallant et al.[9] have used the aforementioned technique to estimate N($^4$S) concentration in an NRP discharge operated in nitrogen at 1 bar from 20-100 µs after the pulse. They reported densities on the order of $10^{15}$ cm$^{-3}$ in this range. However, this technique cannot be used to determine the concentration of N($^4$S) during the discharge.

[1] Postdoctoral Fellow, ciprian.dumitrache@centralesupelec.fr, AIAA Member
[2] PhD Student, arnaud.gallant@centralesupelec.fr
[3] Professor, gabi-daniel.stancu@centralesupelec.fr
[4] Professor, chirstophe.laux@centralesupelec.fr, AIAA Associate Fellow

The main goal of this work is to present a new diagnostic technique, based on femtosecond two-photon absorption laser-induced fluorescence (fs-TALIF), that enables spatially and temporally resolved measurements of ground-state population of atomic nitrogen in an NRP discharge at high pressures ($p \geq 1$ bar). The first nitrogen TALIF experiment was performed by Bischel et al. [10] inside a flow discharge in which atomic nitrogen was obtained by $N_2$ dissociation in a He+$SF_6$ buffer gas mixture at ~10 Torr. Their proposed scheme involved the two-photon excitation of the 3p $^4$D multiplet state at $\lambda = 2 \times 211$ nm with fluorescence collection taking place in the NIR at 868 nm following the radiative decay: 3p $^4$D $\leftarrow$3s $^4P_{5/2}$. In our experiments, we are using a different TALIF excitation scheme involving the 3p $^4S_{3/2}$ level at $\lambda = 2 \times 206.6$ nm. This scheme was first proposed by Adams et al. and it has been shown in the past to present some distinct advantages compared to the scheme proposed by Bischel. Despite the higher photon energy, the 3p $^4S_{3/2}$ state benefits from a lower quenching rate of the upper state by $N_2$ [11]. Moreover, the collection of fluorescence takes place in the visible spectrum ($\lambda = 745$ nm) where the quantum efficiency of the most detectors is notably higher.

Previous work on ns-TALIF showed that it can be successfully employed for studying low pressure discharges ( below several tens of milibars[12]). Above this pressure, quenching of the excited state becomes a major loss mechanism with a time scale even faster than the laser pulse length, i.e. below ns at atmospheric pressure[13]. Therefore, the main challenge of this study is to develop a "quenching free" diagnostic technique in the pressure range of interest (p=1-10 bar) using a femtosecond laser as the excitation source.

In our study, the measurements are calibrated using VUV direct absorption performed in a DC calibration discharge that was characterized on the DESIR beamline at the Synchrotron Soleil facility in Saint Aubin, France. The manuscript focuses primarily on the description of the diagnostic technique and it is organized as follows. Section II discusses the theory behind TALIF measurements and explains how femtosecond excitation can result in quench-free measurements. Section III describes the setup and the experimental procedure used for performing the fs-TALIF experiments. This is followed by Section IV which presents the first measurements of absolute number density using the VUV-calibrated fs-TALIF technique. Finally, Section V is dedicated to conclusions and plans for future work.

## II. Theory & Modeling

The two-photon absorption scheme used in the current work involves the excitation of the 3p $^4S_{3/2}$ level ( $\lambda = 2 \times 206.6$ nm) with the subsequent fluorescence collection taking place from the radiative decay to the 3s $^4$P triplet state around 745 nm. If the fluorescence comes exclusively from the two-photon laser excited state, it can be used to directly probe the ground population of atomic nitrogen ($2p^3$ $^4$S). The main processes taking place during fs-TALIF are presented schematically in Fig. 1 below and include: two-photon absorption, $W_{1,2}^{(2\nu)}$, collisional and radiative decay (presented in Fig. 1 as a single term: $T_{i,j} = Q_{i,j} + A_{i,j}$), photo-ionization, $W_{2,3}^{(i)}$, and stimulated emission, $W_{2,1}^{(2\nu)}$.

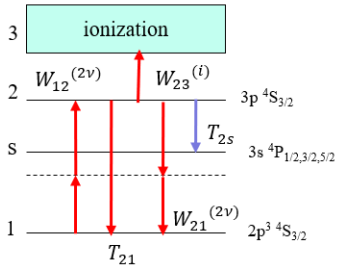


**Figure 1**: Energy level diagram for N-atom TALIF

A 3-level rate model based on the energy level diagram presented above is implemented in order to understand the influence of quenching on the measured signals. The model includes the following rate equations:

$$\begin{aligned} \frac{dN_1}{dt} &= -N_2 W_{12}^{(2\nu)} + N_1 W_{21}^{(2\nu)} \\ \frac{dN_2}{dt} &= N_1 W_{12}^{(2\nu)} - N_2 \left( W_{21}^{(2\nu)} + W_{23}^{(i)} + A_{2s} + Q_{2s} \right) \\ \frac{dN_3}{dt} &= N_2 W_{23}^{(i)} \end{aligned} \quad (1)$$

where the number of fluorescence photons at time t is given by:

$$n_{fl}(t) = \int_0^t A_{2s}\, N_2(t')dt \tag{2}$$

Using Eqs. (1)-(2), one can obtain the time evolution of the fluorescence signal as a function of laser intensity.

In principle, at the high laser fluences that characterizes the femtosecond sources of excitation, the model suggests that it is possible to perform fluorescence measurements that are insensitive to quenching. This is demonstrated in Fig. 2 below by solving Eqs. (1)-(2) for a laser fluence corresponding to 100 GW/cm$^2$. As shown in Fig. 2, during the initial phase of the laser pulse an increase in fluorescence signal is observed. This is due to the increase of population of the 3p $^4S_{3/2}$ excited state. However, after a few tens of femtosecond, the signal begins to decay rapidly such that, by the end of the laser pulse (assumed here a gaussian with FWHM=100 fs), almost 90% of the signal has already vanished. This observed decay is due to the presence of photo-ionization which acts to decrease the population of the excited state 3p $^4S_{3/2}$. If the laser fluence is increased to the point in which the rate of depopulation of the excited state by 2+1 REMPI becomes much stronger than the rate of quenching, the fluorescence decays almost completely by the end of the laser pulse and the measurement becomes unaffected by quenching (which takes place on time scales on the order of picoseconds). A similar result was also indicated by Stancu for oxygen ns-TALIF[14] using the density matrix approach which includes Rabi oscillations and Stark shifts. We should mention that the rate equation approach used here is precise only at low laser intensities. However, Fig. 2 captures qualitatively the significant reduction of the fluorescence time for the high intensity case.

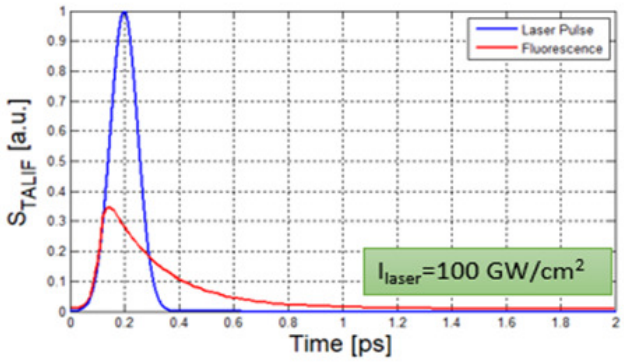


**Figure 2:** Time evolution of modeled fs-TALIF signal for $I_{laser}$=100GW/cm$^2$ at p=1 bar in pure nitrogen.

Still, operating in the high-laser fluence regime causes additional challenges in extracting absolute number densities from the fluorescence signals. Past ns-TALIF measurements were performed in the low excitation regime in which the excited level is only very weakly populated compared to the ground state. In this case, the dominant mechanisms of de-excitation are the decay to the metastable 3s $^4P$ triplet by collisional quenching and radiative decay. A popular method to extract absolute number density information for such an experiment uses krypton gas as a calibration source because it has a similar two-photon absorption cross-section to nitrogen[15–17]. In the femtosecond regime, the transition becomes saturated. Moreover, additional de-population mechanism of the 3p $^4S_{3/2}$ excited state exist, such as: 2+1 REMPI and (possibly) stimulated emission. Under these circumstances, krypton calibration becomes impractical and a new calibration method needs to be devised. The new technique will ideally involve a well-known source of N-atom such that direct quantification of REMPI, two-photon cross-section (itself uncertain in the high laser fluence regime), and stimulated emission can be avoided. For this purpose, a DC discharge operating in nitrogen was developed and characterized using the VUV beamline of a synchrotron. This well-known source will act as a calibration standard for our next measurements of N-atom using fs-TALIF. Under these conditions, the unknown number density of ground state atomic nitrogen inside the NRP discharge is simply related to the number density measured in the DC discharge and the ratio of TALIF signals at the two conditions:

$$n_N = n_{N\_DC}\frac{S_N}{S_{N\_DC}}\frac{\eta_{N\_DC}T_{N\_DC}}{\eta_N T_N}\left(\frac{E_{N\_DC}\nu_N}{E_N\nu_{N\_DC}}\right)^2\frac{\sigma^{(2)}_{N\_DC}}{\sigma^{(2)}_N}\frac{a_{N\_DC}}{a_N} \tag{3}$$

Please note that Eq (3) simplifies to the boxed relationship only as long as the measurement is quench-free such that the ratio of fluorescence quantum yield, $a_{N\_DC}/a_N$, remains the same in both discharges. As discussed earlier, this is holds true only at very high laser intensities.

## III. Experimental Setup

The optical layout used for fs-TALIF experiments shown in Fig. 3 was described in detail previously[18]. Briefly, the excitation femtosecond laser pulse is produced by a Ti:Sapphire laser system (Spectra Physics Solstice ACE) which operates in the wavelength range λ = 780-830 nm. In its current configuration, the Solstice Ace system provides 100 fs pulses with an average pulse power ~7 Watts at a repetition rate of 1 kHz. The output beam of the Ti:Sapphire laser(λ=828nm)is frequency-quadrupled to reach the TALIF wavelength using a third harmonic stage (Spectra Physics TP-1A-THG) followed by a fourth harmonic stage (Spectra Physics TP-1A-FHG). Finally, the excitation wavelength (λ=207 nm) is focused inside of the discharge reactor using an f=100 mm lens and the fluorescence is collected perpendicular to the interrogation region using a spectrometer (Acton SP-500i). The spectrometer entrance slit width was set to 500 microns and the entire slit height is imaged vertically onto the detector array of an ICCD camera (Princeton Instruments PiMax 2). For all the experiments reported here a 1200 grooves/mm grating blazed at 500 nm was used. The dispersion was determined to be 0.034 nm/pixel, which yielded an on-ICCD spectral resolution of 0.43 nm/pixel (pixel size corresponds to $12 \times 24\ \mu m$ for a 512 x 512 pixel array). The camera gain was set to 100% and each set used 30 gates per exposure at a camera nominal repetition rate of 10 Hz. The camera, discharge and laser were synchronized using a pulse delay generator (BNC model 500).

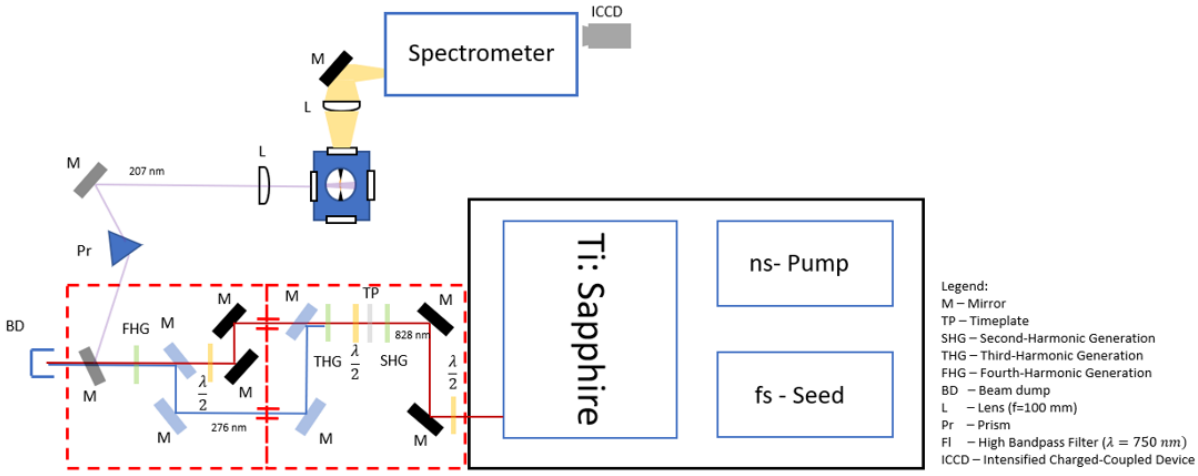


**Figure 3**: Optical Layout for the fs-TALIF experiments. The same setup is used for both Kr calibration and N-atom measurements inside the NRP discharge

NRP discharges are produced with a FID FPG20-30MKS50 high-voltage pulse generator. The generator can deliver pulses of up to 20 kV, with a pulse length tunable between 10-50 ns at a maximum repetition rate of 30 kHz. The maximum current attained in NRP discharges is about 50 A. Presented in Fig. 4 is the electrical diagram of the NRP setup used for electrical measurements (Fig.2-left) and a sample oscillogram (Fig. 4-right). The electric energy is determined by integrating the product of the voltage and current waveforms over the pulse duration. However, the goal is to extract from the total electric energy the amount of energy that is actually deposited into the gas during the discharge. The actual energy deposited is determined as the difference between the incoming and reflected pulse energy (reflection arises due to impedance mismatch at the inter-electrode gap). This method assumes that the losses through heating of the electrodes and radiation (through the electrode antenna) are negligible[19].

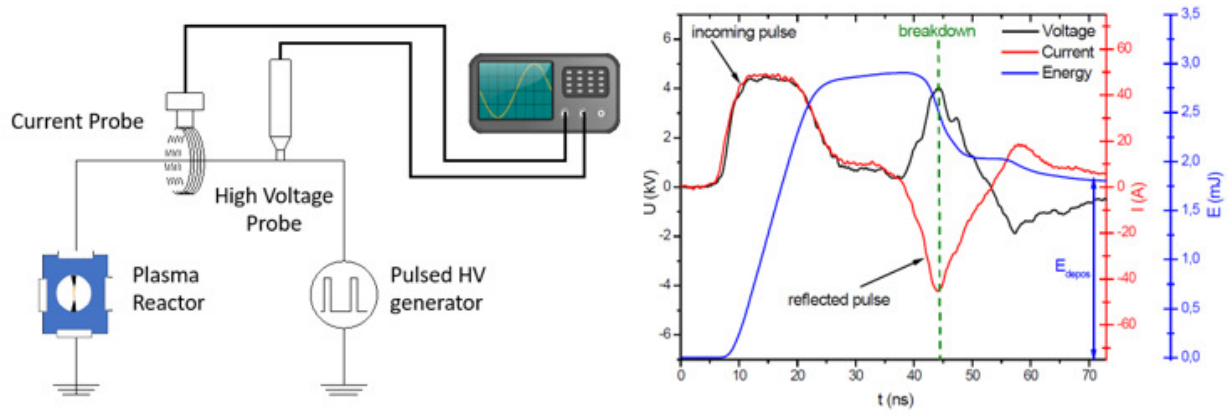


**Figure 4:** (Left) Schematic of the experimental setup used for electrical measurements in NRP discharges. (Right) Sample oscillogram showing the current and voltage measured by the probes as well as the calculated electrical energy. The probes were placed in the middle of a 75 Ω cable.

The DC discharge which was used as a calibration source for the fs-TALIF experiment was built as a glass cell of 10 cm in length (inter-electrode distance) and 1-inch in diameter. The cell offers optical access for the VUV probing beam along the discharge length using a pair of $MgF_2$ windows with a thickness of 1 mm. The same ports are also used during the TALIF calibration procedure for passing the laser beam. The fluorescence is collected from the center of the glass cell through a 1-inch quartz window (5 mm thickness). The discharge was operated at the Soleil Synchrotron facility (shown schematically in Fig. 5 below) over a wide range of conditions: $p_0$=1-10 mbar, Ar:$N_2$ mixtures with dilution factors from 1-3000, $V_{DC}$=0.7-1.5 kV, $I_{DC}$=10-50 mA. The cell was actively cooled using water that was circulated through a copper pipe placed on the outside surface of the cell and around the electrodes. The glass surface temperature was monitored throughout the experiments using a wire thermocouple and did not exceed 150 ºC . The absorption spectra was obtained using the unique VUV Fourier-transform spectrometer (FTS) that is installed on the DESIR beamline at Synchrotron Soleil[20]. Briefly, the spectrometer was developed to cover the VUV spectral range up to λ=40 nm. This instrument coupled with the undulator-based DESIRS beamline allows the recording of high-resolution absorption spectra with a resolving power as high as $\lambda/\Delta\lambda = 10^{16}$. For the tests performed as part of this study, the measured instrumental function corresponded to $\Delta_I = 0.46$ cm$^{-3}$ (FWHM).

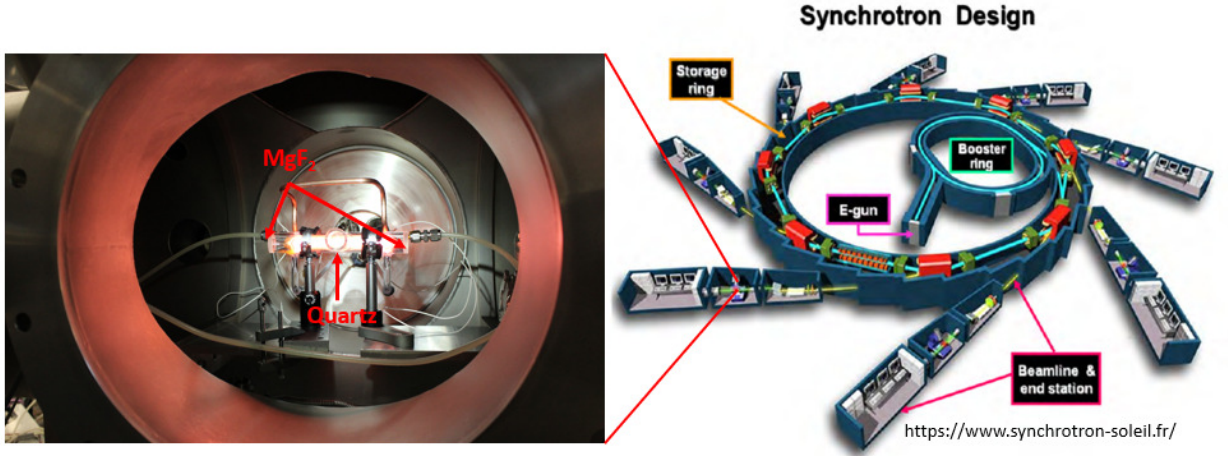


**Figure 5:** (Left) Image of the DC calibration cell inside of the DESIR VUV beamline. (Right) The Soleil synchrotron facility design.

## IV. Results and Discussions

### A. Characterization of the DC discharge

To extract absolute number densities from the fs-TALIF experiment, the DC glass reactor was first characterized inside of the synchrotron facility. The purpose of the DC reactor is to provide a steady, homogenous and reproducible source of atomic nitrogen that can be measured both by direct absorption inside the synchrotron and later by fs-TALIF at the EM2C laboratory. The glass cell length, pressure and operating voltage/current were chosen in order to ensure that the amount of nitrogen dissociation is sufficiently elevated to enable measurement in both absorption and fluorescence. For the absorption experiment, the lowest energy transition that allows probing of the fundamental state was chosen. This corresponds to $N(^4S)\rightarrow N(^4P_{1/2,3/2,5/2})$ at around $\lambda$=120 nm (more spectral information regarding this transition is given in Table 1 below). The detection limit for the VUV absorption was estimated beforehand by performing a direct absorption simulation using Beer-Lambert's law:

$$T(\lambda) = exp[-A(\lambda)] = exp[-k(\lambda) \cdot l_{abs}] \tag{4}$$

Where the absorption coefficient for each of the three absorption lines, $k_i$ (i=1÷3), corresponds to:

$$k_i = \frac{e^2}{4\varepsilon_0 m_e c} f_i \cdot \left[n_{N(4S)}\right] \tag{5}$$

Here, e is the electron charge, $\varepsilon_0$ is the permitivitty of free space, $m_e$ is the electron mass, c is the speed of light and $f_i$ is the oscillator strength (taken from NIST atomic database[21]). The collected spectrum, $I_T(\lambda)$, represents a convolution between the transmission spectrum, $T(\lambda)$, and the FTS instrument function, $\varphi_{instr}(\lambda - \lambda_0)$:

$$I_T(\lambda) = I_0(\lambda)[T(\lambda) \otimes \varphi_{instr}(\lambda - \lambda_0)] \tag{6}$$

Where $I_0(\lambda)$ represents the reference spectrum intensity without the absorption which is determined experimentally by fitting the synchrotron undulator shape.

**Table 1:** Spectroscopic data for the VUV absorption investigated experimentally at Soleil Synchrotron

| Wavelength [nm] | Oscillator Strength | Lower Level, Term, J | Upper Level, Term, J |
|---|---|---|---|
| 119.96 | 1.32e-01 | $2s^22p^3$, $^4S°$, 3/2 | $2s^22p^2(^3P)3s$, $^4P$, 5/2 |
| 120.02 | 8.69e-02 | $2s^22p^3$, $^4S°$, 3/2 | $2s^22p^2(^3P)3s$, $^4P$, 3/2 |
| 120.07 | 4.32e-02 | $2s^22p^3$, $^4S°$, 3/2 | $2s^22p^2(^3P)3s$, $^4P$, 1/2 |

The simulated absorption spectra are shown in Fig. 6 below for a wide range of atomic nitrogen number density. The simulation is used to estimate the range of sensitivity of our VUV absorption measurement. For an absorption path length of 10 cm, assumed discharge temperature T=300 K and an instrument function $\Delta_I = 0.5$ cm$^{-3}$, the simulation shows that the peaks become saturated for number densities above $10^{13}$ cm$^{-3}$. Alternatively, the limit of detection is estimated to be around $5 \times 10^{10}$ cm$^{-3}$ for an assumed noise level of 5% on the background.

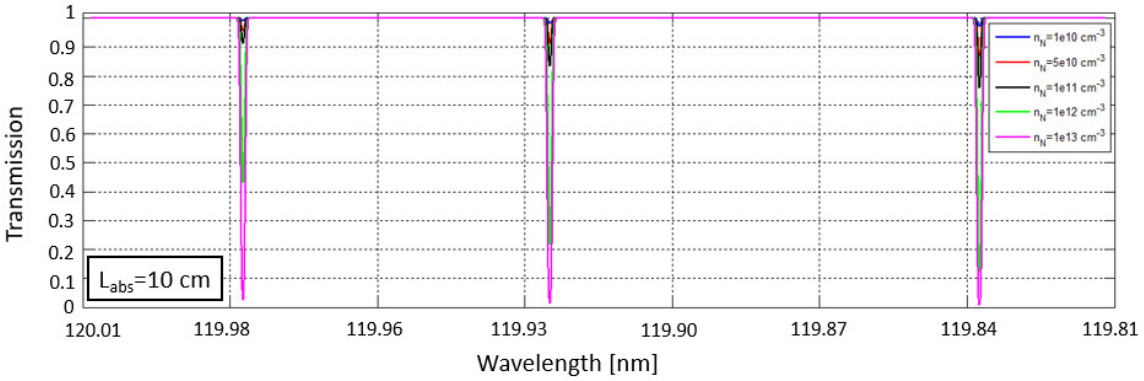


**Figure 6:** Simulated absorption spectra for various atomic nitrogen densities. The simulation assumes an absorption length of 10 cm, T=300 K and instrument function $\boldsymbol{\Delta_I = 0.5}$ cm$^{-3}$ (FWHM).

Experimental results for the VUV absorption measurements are provided in Fig. 7 for a mixture of Ar:$N_2$ (3000:1 dilution) at p=1 mbar, T=400 K. The discharge was operated at a current of 5 mA and a voltage corresponding to 0.8 kV. Since the ground state does not show splitting, any of the three transitions can be used to measure concentration of N($^4$S) (the best fit for each of the three lines shown in Fig. 7 below). However, this is never the case in reality and the three peaks can be used to determine the uncertainty of the measurement. Under this particular configuration the number density was estimated to be: $n_{N(4S)}=7.66\pm0.84$ x $10^{11}$ cm$^{-3}$. Where the error of 11.5% comes primarily from the uncertainty given by the best fit of each of the three peaks. Other parameters that play into the uncertainty are the precision of the fit (accounts for less than 3%) and shot noise (~5% after averaging over 50 scans, with each complete scan taking 5-10 minutes).

For fs-TALIF calibration this number density was below our detection limit. As such the dilution factor was reduce to Ar:N2=14:1, and the discharge current was increased to 10 mA to yield a number density of $2.5\pm0.27$ x $10^{13}$ cm$^{-3}$. To better asses the uncertainty of the path-integrated direct absorption measurement, the length of the absorption column and the radial profile of atomic nitrogen in the discharge were determined experimentally by translating the cell with respect to the TALIF beam in both radial direction and along the optical axis of the fs-laser. This gave an uncertainty of 10% in the measured number density along a radial distance of $\pm$ 5 mm (this measurement was important because the VUV beam was 5 x 2 mm in size and the FTS instrument does not allow for spatially resolved absorption profiles) and 15% variation along the integrated pathlength. Moreover, the true absorption path was determined using fs-TALIF to be 11 cm in length. The detection limit of the fs-TALIF setup was also determined during this phase using the signal-to-noise ratio on each of the three observed fluorescence peaks. In the conditions described above for the DC discharge ($n_{N(4S)}=2.5\pm0.27$ x $10^{13}$ cm$^{-3}$), the fs-TALIF signals measured inside the discharge yield a $SNR_{746}$=17.5, $SNR_{744}$=10, $SNR_{742}$=5. This corresponds to a detection limit of ~ $10^{12}$ cm$^{-3}$, two orders of magnitude lower than previously reported for ns-TALIF[16,17,22].

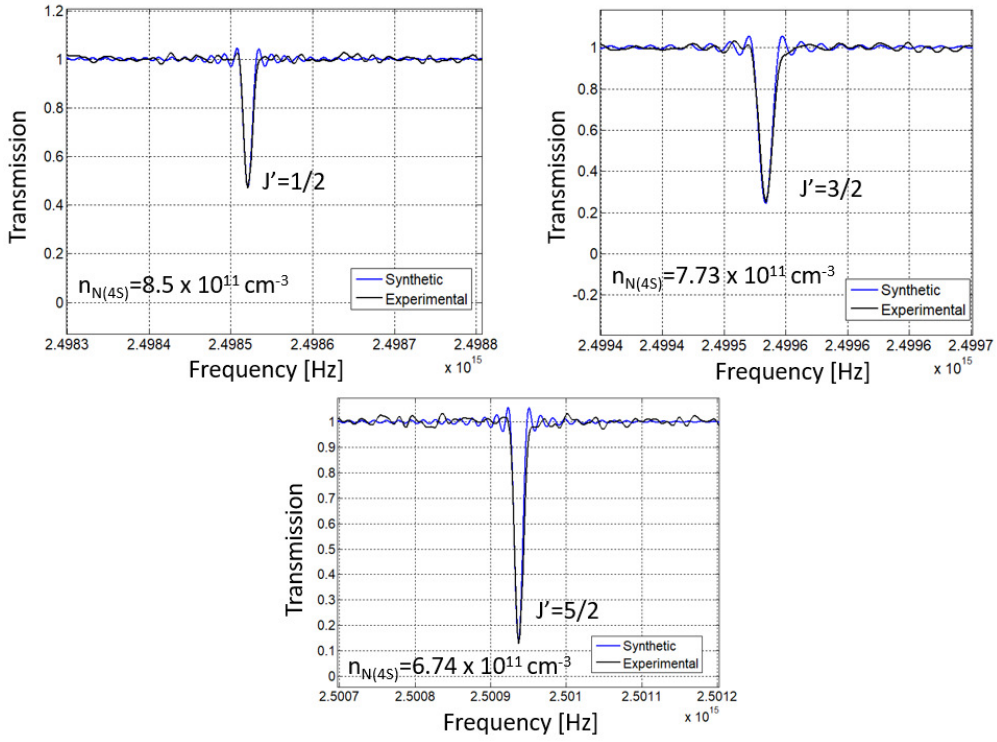


**Figure 7:** VUV Transmission spectra for the transition N($^4$S)→N($^4P_{1/2,3/2,5/2}$) around λ=120 nm. Best fit for each peak is determined and subsequently used to determine the uncertainty of the N($^4$S) number density.

### B. Fs-TALIF calibration & Detection limit

The fs-TALIF technique (calibrated using the reference density from the DC-discharge) is subsequently used to determine the number density of atomic nitrogen generated in an NRP discharge operated at $p_0$=1bar, $T_0$=300 K, 10

Hz, pin-to-pin distance of 1 mm, and 10 ns discharge pulse length. The time evolution of the atomic number density in the post-discharge is shown in Fig. 8 from 1-500 µs. The maximum number density corresponds to ~$5 \times 10^{16}$ $cm^{-3}$ at 1 µs. During the first 10 µs, a very sharp decrease is noted. This is believed to be caused by the hydrodynamic effects that were previously observed in the discharge at early times which makes the plasma expand very quickly as it cools down [23]. Between 10-60 µs the number density stays relatively constant throughout. Over this range of time delays, the recombination is counter-balanced by the increase in ground state population through collisional de-excitation of atomic nitrogen excited states ($N(^2P)$, $N(^2D)$ and $N(^4D)$,in particular) [24,25]. Hydrodynamically, we also observe a kernel compression (which ultimately leads to a collapse of the kernel into a torus) during this time. This compression could also explain the observed trend during this stage. For t > 60 µs, one notes a gradual decrease in ground state atomic nitrogen in the post-discharge which is believed to be caused by three-body recombination of atomic nitrogen to form $N_2(B)$[24,26,27]. In fact, OES measurements tracking the evolution of the first positive (in particular, $N_2(B,v=11)$) in the post-discharge were observed to correlate very well with the fs-TALIF measurements performed in this work. The error bars observed in Fig. 8 come primarily from shot-noise. Other possible sources of uncertainty were investigated, such as: variability in electrode radius (different sets of electrodes were tested), discharge voltage (the voltage was varied by ±10 % of the nominal value), and mixture pressure (pressure was varied within 10% of nominal value) but such changes were observed to be below the uncertainty induced by the shot-noise. This indicates that the precision of the reported results could be further increased by augmenting the collection time.

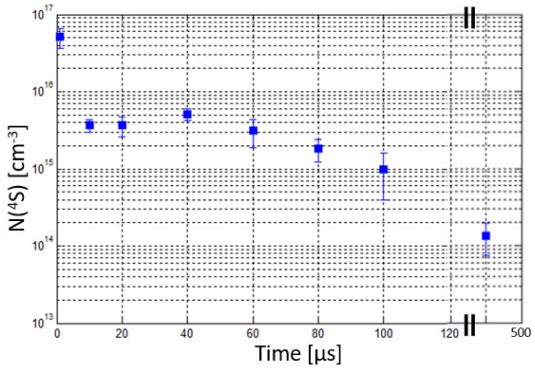


**Figure 8:** Atomic nitrogen TALIF signal evolution in time for various pressures inside of an NRP discharge ($V_{disch}$=15 kV)

The highest pressure in which fs-TALIF signal was collected so far corresponds to 5 bar and was limited by the window thickness on the reactor and the ability to supply the voltage required to generate breakdown at higher pressures. As shown from Fig. 9, all three transitions of the triplet are still visible at 5 bars and the signal-to-noise level is still reasonably high at 5 bars ($SNR_{742nm}$=6.7, $SNR_{744nm}$=14,$SNR_{746nm}$=31.4) indicating that it is possible to further increase the pressure once the chamber is adapted for higher pressure operation and the pulse voltage is augmented.

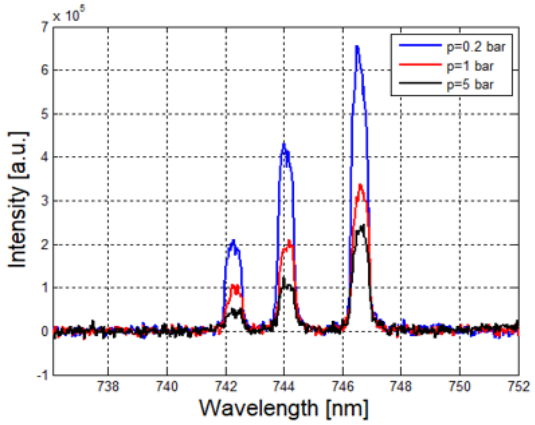


**Figure 9:** Fluorescence signal for atomic nitrogen at three different pressures ($V_{disch}$=15 kV).

## V. Conclusions and Future Work

The main objective of this contribution was to develop a quench-free diagnostic technique which would allow measurements of ground state atomic nitrogen at high-pressure with high spatial and temporal resolution. Under these conditions neither direct absorption spectroscopy (lacks spatial resolution) nor typical ns-TALIF (quenching rate is too high at pressures above 100 mbar) provide satisfactory results. The fs-TALIF scheme developed here involves the excitation of the $3p\ ^4S_{3/2}$ level ($\lambda = 2 \times 206.6$ nm) with the subsequent fluorescence collection taking place from the radiative decay to the $3s\ ^4P$ triplet state around 745 nm. To extract absolute number densities from the fluorescence measurements a new calibration technique based on VUV direct absorption spectroscopy was investigated. The VUV measurements were performed at the synchrotron Soleil facility inside of a DC glass cell which was designed to operate over a wide range of conditions (p=0.1-10 mbar, I=1-50 mA). We showed that atomic nitrogen densities as low as $10^{11}$ $cm^{-3}$ were successfully measured in the synchrotron with an uncertainty of ~10% (which resulted mainly from the density predicted by each of the three peaks around 120 nm).

For the fs-TALIF experiments, a limit of detection of $10^{12}$ $cm^{-3}$ was determined based on the calibration data provided by the VUV measurements. Moreover, absolute number densities are reported for the first time using our technique. These measurements were performed inside of an NRP discharge operating at 1 bar in a nitrogen mixture. It is important to note that, at this stage, the quench-free regime was only postulated using the 3-level rate equation model. However, future work will attempt to experimentally test whether this assumption holds true under the conditions investigated here. Finally, the femtosecond excitation regime presents some interesting opportunities (such as developing a quench-free diagnostic) but also presents a series of challenges: uncertainty regarding the two-photon cross section due to Rabi oscillations and Start shifting of the lines, presence of 2+1 REMPI and (possibly) stimulate emission. Future work will focus on evaluating the contribution of each of these processes to the collected fluorescence.


## Acknowledgements

This research was funded by the French National Research Agency, ANR, Project ASPEN ANR-16-CE30-0004 and IdF-SESAME, project DIAGPLAS. The authors would also like to acknowledge Dr. N. de Oliveira and Dr. L. Nahon for their assistance with the VUV absorption experiments that were conducted at Synchrotron Soleil (Saint Aubin, France).


## References


1 Cho, C., Kinemuchi, Y., Suematsu, H., Jiang, W., and Yatsui, K., "Enhancement of nitridation in synthesis of aluminum nitride nanosize powders by pulsed wire discharge," *Japanese Journal of Applied Physics, Part 1: Regular Papers and Short Notes and Review Papers*, vol. 42, 2003, pp. 1763–1765.

2 Pai, D. Z., Ostrikov, K. K., Kumar, S., Lacoste, D. A., Levchenko, I., and Laux, C. O., "Energy efficiency in nanoscale synthesis using nanosecond plasmas," *Scientific Reports*, vol. 3, 2013, pp. 1–7.

3 Noli, F., Pichon, L., and Öztürk, O., "The Influence of Plasma-Based Nitriding and Oxidizing Treatments on the Mechanical and Corrosion Properties of CoCrMo Biomedical Alloy," *Metallurgical and Materials Transactions A: Physical Metallurgy and Materials Science*, vol. 49, 2018, pp. 1383–1396.

4 Liu, R., Li, X., Hu, X., and Dong, H., "Surface modification of a medical grade Co-Cr-Mo alloy by low-temperature plasma surface alloying with nitrogen and carbon," *Surface and Coatings Technology*, vol. 232, 2013, pp. 906–911.

5 Uddi, M., Jiang, N., Adamovich, I. V., and Lempert, W. R., "Nitric oxide density measurements in air and air/fuel nanosecond pulse discharges by laser induced fluorescence," *Journal of Physics D: Applied Physics*, vol. 42, 2009.

6 Sun, W., and Ju, Y., "Nonequilibrium Plasma-Assisted Combustion: A Review of Recent Progress," *J. Plasma Fusion Res.*, vol. 89, 2013, pp. 208–219.

7 Niemi, K., O'Connell, D., De Oliveira, N., Joyeux, D., Nahon, L., Booth, J. P., and Gans, T., "Absolute atomic oxygen and nitrogen densities in radio-frequency driven atmospheric pressure cold plasmas: Synchrotron

vacuum ultra-violet high-resolution Fourier-transform absorption measurements," *Applied Physics Letters*, vol. 103, 2013, pp. 1–5.

[8] Salmon, A., "Diagnostics and kinetics of reactive oxygen and nitrogen species in atmospheric pressure non-equilibrium discharges for bio-decontamination," CentraleSupelec, 2018.

[9] Gallant, A., Dumitrache, C., Stancu, G., and Laux, C., "Long-lived emission in the afterglow of Nitrogen NRP discharges : a tool for hydrodynamics and kinetics studies," *24th International Symposium on Plasma Chemistry*, Naples: 2019.

[10] Bischel, W. K., Perry, B. E., and Crosley, D. R., "Two-photon laser-induced fluorescence in oxygen and nitrogen atoms," *Chemical Physics Letters*, vol. 82, 1981, pp. 85–88.

[11] Adams, S. F., and Miller, T. A., "Two-photon absorption laser-induced fluorescence of atomic nitrogen by an alternative excitation scheme," *Chemical Physics Letters*, vol. 295, 1998, pp. 305–311.

[12] Dobele, H. F., Mosbach, T., Niemi, K., and Schulz-Von Der Gathen, V., "Laser-induced fluorescence measurements of absolute atomic densities: Concepts and limitations," *Plasma Sources Science and Technology*, vol. 14, 2005.

[13] Agrup, S., Ossler, F., and Aldén, M., "Measurements of collisional quenching of hydrogen atoms in an atmospheric-pressure hydrogen oxygen flame by picosecond laser-induced fluorescence," *Applied Physics B Lasers and Optics*, vol. 61, 1995, pp. 479–487.

[14] Stancu, G. D., "Laser based spectroscopic diagnostics from UV to Mid-IR applied to the study of atmospheric pressure discharges," *Spectroscopy and Spectroscopic: measurement techniques for aerospace flows*, D. Giordano and Y. Babou, eds., Von Karman Institute, 2014.

[15] Niemi, K., Schulz-von der Gathen, V., and Dobele, H. F., "Absolute calibration of atomic density measurements by laser-induced fluorescence spectroscopy with two-photon excitation," *Journal of Physics D: Applied Physics*, vol. 34, 2001, pp. 2330–2335.

[16] Niemi, K., Gathen, V. S. der, and Döbele, H. F., "Absolute atomic oxygen density measurements by two-photon absorption laser-induced fluorescence spectroscopy in an RF-excited atmospheric pressure plasma jet," *Plasma Sources Science and Technology*, vol. 14, 2005, pp. 375–386.

[17] Es-Sebbar, E. T., Sarra-Bournet, C., Naud́, N., Massines, F., and Gherardi, N., "Absolute nitrogen atom density measurements by two-photon laser-induced fluorescence spectroscopy in atmospheric pressure dielectric barrier discharges of pure nitrogen," *Journal of Applied Physics*, vol. 106, 2009.

[18] Dumitrache, C., Gallant, A., Stancu, G. D., and Laux, C. O., "Femtosecond Two-Photon Absorption Laser Induced Fluorescence (fs-TALIF) Imaging of Atomic Nitrogen in Nanosecond Repetitive Discharges," *AIAA 2019-1507*, 2019, pp. 1–11.

[19] Maly, R., and Vogel, M., "Initiation and propagation of flame fronts in lean CH4-air mixtures by the three modes of the ignition spark," *Symposium (International) on Combustion*, vol. 17, 1979, pp. 821–831.

[20] De Oliveira, N., Joyeux, D., Phalippou, D., Rodier, J. C., Polack, F., Vervloet, M., and Nahon, L., "A Fourier transform spectrometer without a beam splitter for the vacuum ultraviolet range: From the optical design to the first UV spectrum," *Review of Scientific Instruments*, vol. 80, 2009.

[21] Kramida, A., Ralchenko, Yu., Reader, J., "NIST Atomic Spectra Database," *National Institute of Standards and Technology* Available: http://physics.nist.gov/asd.

[22] Es-sebbar, E., Benilan, Y., Jolly, A., and Gazeau, M.-C., "Characterization of an $N_2$ flowing microwave post-discharge by OES spectroscopy and determination of absolute ground-state nitrogen atom densities by TALIF," *Journal of Physics D: Applied Physics*, vol. 42, 2009, p. 135206.

[23] Stepanyan, S., Minesi, N., Salmon, A., Stancu, G. D., and Laux, C. O., "Spatial evolution of the plasma kernel produced by nanosecond discharges in air," *J. Phys. D Appl. Phys*, 2019, pp. 1–17.

[24] Popov, N. A., "Dissociation of nitrogen in a pulse-periodic dielectric barrier discharge at atmospheric

pressure," *Plasma Physics Reports*, vol. 39, 2013, pp. 420–424.

[25] Volynets, A. V, Lopaev, D. V, Chukalovsky, A. A., Mankelevich, Y., and Popov, N. A., "N 2 dissociation and kinetics of N( 4 S) atoms in nitrogen DC glow discharge Alternative approaches for ultra low-k materials integration View project Advanced Interconnects View project," *Article in Journal of Physics D Applied Physics*, vol. 51, Sep. 2018, p. 364002.

[26] Levaton, J., Amorim, J., Souza, a R., Franco, D., and Ricard, a, "Kinetics of atoms, metastable, radiative and ionic species in the nitrogen pink afterglow," *Journal of Physics D: Applied Physics*, vol. 35, 2002, pp. 689–699.

[27] Amorim, J., "Lewis – Rayleigh and Pink Afterglow," *IEEE Transactions on Plasma Science*, vol. 33, 2005, pp. 368–369.